AFRL-VS-HA-TR-98-0124

MODELING INFRARED GLOW ABOVE THUNDERSTORMS

Peter P Wintersteiner

ARCON Corporation
260 Bear Hill Rd
Waltham, MA 02451-1080

23 Dec 1998

Scientific Report No. 1
April 1996-Mar 1997

AIR FORCE RESEARCH LABORATORY
Space Vehicles Directorate
29 Randolph Rd
AIR FORCE MATERIEL COMMAND
Hanscom AFB, MA 01731-3010

This technical report has been reviewed and is approved for publication.

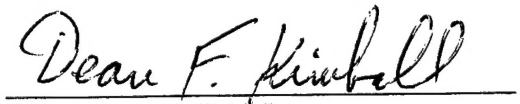

DEAN F. KIMBALL
Contract Manager
AFRL/VSSS

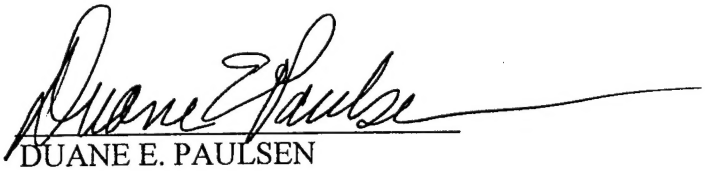

DUANE E. PAULSEN
Deputy Chief
AFRL/VSSS

This report has been reviewed by the ESC Public Affairs Office (PA) and is releasable to the National Technical Information Service (NTIS).

Qualified requestors may obtain additional copies from the Defense Technical Information Center (DTIC). All others should apply to the National Technical Information Service (NTIS).

If your address has changed, if you which to be removed from the mailing list, or if the addressee is no longer employed by your organization, please notify AFRL/VSIM, 29 Randolph Road, Hanscom AFB MA 01731-3010. This will assist us in maintaining a current mailing list.

Do not return copies of this report unless contractual obligations or notices on a specific document require that it be returned.

REPORT DOCUMENTATION PAGE

Form Approved
OMB NO. 0704-0188

1. AGENCY USE ONLY (Leave Blank)	2. REPORT DATE	3. REPORT TYPE AND DATES COVERED
	22 October 1998	Scientific Report #1 4 April 1996—31 March 1997

4. TITLE AND SUBTITLE
Modeling Infrared Glow above Thunderstorms

5. FUNDING NUMBERS
F19628-96-C-0048
PE 61102F
PR 2310
TA GD
WU AP

6. AUTHOR(S)
Peter P. Wintersteiner

7. PERFORMING ORGANIZATION NAME(S) AND ADDRESS(ES)
ARCON Corporation
260 Bear Hill Rd.
Waltham, MA, 02451-1080

8. PERFORMING ORGANIZATION REPORT NUMBER

9. SPONSORING / MONITORING AGENCY (S) NAME AND ADDRESS(ES)
Air Force Research Laboratory
Hanscom AFB, MA 01731-3010
Contract Manager: Dean Kimball/VSSS

10. SPONSORING / MONITORING AGENCY REPORT NUMBER
AFRL-VS-HA-TR-98-0124

11. SUPPLEMENTARY NOTES

12 a. DISTRIBUTION / AVAILABILITY STATEMENT
Approved for Public Release; Distribution Unlimited

12 b. DISTRIBUTION CODE

13. ABSTRACT (Maximum 200 words)

An investigation of the effect of thundercloud charging on electric fields in the middle atmosphere has led to the prediction that heating of electrons in the D-region should occur over time scales of minutes or longer. We have studied the effect of this heating on the excitation of vibrational states of N_2 and CO_2. Because of the quasi-steady nature of the excitation, it is possible to perform radiative-transfer calculations and determine that populations of the infrared-active ν_3 states of CO_2 are substantially enhanced in the region at and above 75 km, given a charge distribution of sufficient magnitude in the upper troposphere. The resulting infrared "glow" is predicted to be as much as 100% above the limb background in such cases. MWIR sensors can therefore be expected to measure increased radiance in the CO_2 bands when viewing the mesosphere in the vicinity of very large thunderstorm complexes. The limited spatial extent of the excitation will also result in enhanced MWIR radiance structure.

14. SUBJECT TERMS
Infrared emission; infrared glow; thunderstorms; sprites; CO_2 4.3 μm; MWIR structure; ARC; electron heating

15. NUMBER OF PAGES
8

16. PRICE CODE

17.SECURITY CLASSIFICATION OF REPORT	18.SECURITY CLASSIFICATION OF THIS PAGE	19.SECURITY CLASSIFICATION OF ABSTRACT	20.LIMITATION OF ABSTRACT
Unclassified	Unclassified	Unclassified	Unlimited

This Scientific Report summarizes some of the research that has been carried out under the provisions of contract #F19628-96-C-0048 during the twelve months ending in March 1997. Our report is accompanied by reprints of a paper, entitled "Infrared Glow Above Thunderstorms?", that appeared in *Geophysical Research Letters* late in 1997. This paper gives a complete description of the work in question. It resulted from a collaboration of the non-LTE research groups at ARCON and AFRL on the one hand, and the thunderstorm electrification group at the STAR Laboratory of Stanford University on the other. This Report gives a summary of the completed work and ARCON's role in completing it.

The research reported here concerns infrared emissions in the upper mesosphere, specifically MWIR emissions of CO_2. These emissions contribute substantially to the natural signature of the atmosphere at all times. We concluded that such emissions also are likely to be induced by charge distributions that exist in clouds within large thunderstorm complexes known as mesoscale convective complexes (MCCs), and predict that such emissions not only exist as a quasi-steady state condition but also are sufficiently above background levels to be detectable from space.

BACKGROUND

Much attention has been devoted in the past three or four years to transient optical emissions that have been associated with powerful cloud-to-ground lightning strokes, and that have been given various names such as "sprites", and "upward-propagating lightning". These emissions are understood to result from the excitation of optically-active states by electron impact, free electrons being momentarily heated to temperatures well in excess of ambient temperatures by electric fields induced by the sudden redistribution of charge in the clouds and ground at the time of the lightning stroke. The most spectacular manifestation of this phenomenon appears at visible wavelengths, mostly in the red. But there is also great interest in the infrared signature of such events, which has led to our participation in research efforts to model it.

With a sufficiently powerful stroke, the impacts of the heated electrons deposit a significant amount of energy in the N_2 vibrational reservoir, which is easily excited by electron impact and which also readily transfers energy to infrared-emitting states of CO_2. We have modeled this process, and also the effect of direct electron impact upon CO_2, in order to estimate the emission rates and determine whether a signature of such events can be expected to be seen above background. The problem is a very difficult one to solve quantitatively, because the volume emission is not only transient but also spatially limited, requiring that radiative transfer codes used to deal with the optically-thick emissions be specifically adapted to these conditions. We have made some progress in this adaptation, at least in the direction of dealing with transients. Although a quantitative solution has not been realized, it is clear that observation of such emissions from the ground is precluded by the great optical depth at 4.3 μm. Observation from space is another question, one that remains open at this time.

INFRARED GLOW

The work discussed in the accompanying *GRL* paper is based upon the realization that the quasistatic electric fields above charged thunderclouds should also heat the ambient electrons in the D region to some extent. This provides an additional potential excitation mechanism, having a much broader spatial extent and a much longer duration than the discharge process that produces sprites, one that can be expected to produce a steady enhancement or "glow" in the infrared. That is, with time scales on the order of a minute or more (rather than milliseconds characteristic of discharges) and spatial structures on the order of many tens of kilometers, calculations assuming a quasi-steady state and the absence of horizontal spatial structure provide a viable description of the radiative transfer. Together with the electron heating and other excitation and de-excitation processes, the radiative transfer rates determine the population of the infrared-active vibrational states and the resulting volume emission. Having the capability of performing such calculations using the AFRL Atmospheric Radiance Code (ARC), we therefore engaged in a program to quantify the problem.

CALCULATIONS

The extent of the electron heating was determined using a two-dimensional self-consistent quasi-electrostatic heating model developed by Inan and co-workers at Stanford. Assuming various charge distributions at cloud and ground level, certain parameterizations of the free-electron density or atmospheric conductivity in the D region, and cylindrical symmetry, it is possible to derive the electrostatic field. This is used in a kinetic model, which includes loss due to vibrational excitation of N_2, to determine an electron distribution function and the vibrational excitation rate for N_2. This excitation rate is used, together with assumptions about the condition of the background atmosphere, to run the ARC model and determine the vibrational temperatures of all the important IR-active states of CO_2 (as well as that of the IR-inactive N_2) as a function of altitude. The ARC model was specifically adapted to make use of this particular sort of excitation. We then calculated the limb radiance that would be detected by a space-borne sensor looking above a region with thunderstorm activity.

The enhanced quasi-steady state heating is important in the upper mesosphere, at altitudes between approximately 65 and 85 km. At lower altitudes the free-electron density is too small to produce much of an effect, and at higher altitudes the collision rate is small. Incorporating the enhanced production of N_2 vibration in our model, we determined the vibrational temperatures of the primary MWIR-emitting CO_2 states, 00011 and 01111, and also the higher-lying "Group-1" states, 10012, 02211, and 10011. We did this (for the four most abundant isotopes of CO_2) for several cases, incorporating different assumptions about the charge distributions and atmospheric conductivity and specifying nighttime background conditions. (If this phenomenon does occur in daytime, the solar-pumped IR ambient background would overwhelm any signal it would produce.)

The results were quite different for the different assumed conditions. When a low conductivity or a modest-sized charge (100 C) is assumed, the extra energy input is not sufficient to raise the vibrational temperatures and populations of the N_2 and CO_2 states. When a much larger, but still realistic, charge (1000 C) is assumed, the vibrational

temperatures are significantly elevated at altitudes above 75 km. The most dramatic effect is on the 626-00011 state, which is the most copious emitter of 4.3 μm photons. The electrostatic heating manifests itself as a peak in the vibrational temperature at about 80 km that is almost 50 K above the ambient profile in the strongest case. Moreover, the temperature is somewhat elevated at all altitudes above 80 km, even where the direct effect of the heating is negligible, because of increased upwelling radiation from the 80-km region. There are similar but smaller enhancements in the 00011 minor-isotope populations and those of the second ν_3 excited state (01111), while there is little effect on the Group 1 populations.

The calculation of limb radiance was carried out using a recent improvement to the NLTEA code, which is a component of ARC. We assumed a space-to-space line-of-sight (LOS) passing directly over an active mesoscale convective complex (MCC), and we assumed that the charge distribution was centered below the tangent point, or alternatively at other locations nearer and farther from the observing instrument than the tangent point. Since, for even the most extensive charge distributions (100 or 200 km across), most of the LOS would pass above unperturbed regions, it was necessary to use the enhanced vibrational temperatures over only a portion of the path and vibrational temperatures calculated for ambient nighttime conditions for the remainder. The capability to accommodate spatial structure of various sorts was built into NLTEA, and the calculations for these cases were carried out with ease.

The calculations show that, for the largest charge distribution we assumed, observed limb radiance in the 4.3 μm region would be increased by as much as 100% for tangent paths above 75 km. For the large charge distribution and a smaller conductivity, we predict enhancements of ~20%. These estimates assume the MCC is located directly beneath the tangent points. For distributions nearer to or farther from the observer, the enhancements would be greater or smaller, respectively, due to the smaller or greater optical path from the observer to the heated region. The calculations also show that while the major-isotope fundamental band radiance enhancement is much greater than that for other bands, most of the observed increase would in fact be due to minor-isotope fundamentals. The reason for this is that the 626 fundamental is severely self-absorbed on limb paths through the mesosphere, and other bands therefore contribute relatively more strongly.

CONCLUSIONS

The significant conclusion that can be drawn from this work is that exoatmospheric MWIR sensors can be expected to measure increased radiance in the CO_2 bands when viewing the mesosphere in the vicinity of very large active thunderstorm complexes. The ambient radiance in the absence of thunderclouds already reveals a certain amount of spatial structure due to temperature and density fluctuations, but generally in these bands the variations are smaller than what our calculations are predicting, at least at spatial scales on the order of the tens of kilometers that are at issue here. Therefore, MCCs may prove to be an important source of structure in MWIR radiance.

GEOPHYSICAL RESEARCH LETTERS, VOL. 24, NO. 21, PAGES 2635-2638, NOVEMBER 1, 1997

Infrared glow above thunderstorms?

R. H. Picard,[1] U. S. Inan,[2] V. P. Pasko,[2] J. R. Winick,[1]
and P. P. Wintersteiner[3]

Abstract. Sustained heating of lower ionospheric electrons by thundercloud fields, as recently suggested by *Inan et al.* [1996], may lead to the production of enhanced infrared (IR) emissions, in particular 4.3-μm CO_2 emission. The excitation rate for $N_2(v)$ via electron collisions is calculated using a new steady-state two-dimensional electrostatic-heating (ESH) model of the upward coupling of the thundercloud (TC) electric fields. The vibrational energy transfer to CO_2 and 4.3-μm radiative transfer are then computed using a line-by-line non-LTE (non-local thermodynamic equilibrium) radiation model. Limb-viewing radiance profiles at 4.3-μm and typical radiance spectra are estimated for five different TC charge distributions and ambient ionic conductivities. Broadband 4.3-μm enhancements of greater than a factor of two above ambient nighttime levels are predicted for tangent heights (TH) in the range ~80 to >130 km for the most perturbed case, with larger enhancements in selected narrower spectral regions. The predicted IR enhancements should be observable to an orbiting IR sensor.

Introduction

Thunderstorms are thought to be the batteries for the global electric circuit [*Hays and Roble*, 1979; *Roble*, 1991]. Intense quasi-electrostatic (QE) TC fields which exist during brief (~10 ms) periods following lightning discharges are now believed to heat the free electrons at 50-90 km altitude, leading to the production of new molecular excitation and optical emissions (sprites) [*Pasko et al.*, 1997]. In addition to the visible and near-IR emission from short-lived states, notably N_2 first-positive emission [*Mende et al.*, 1995; *Hampton et al.*, 1996], which are efficiently produced by the transient QE heating, the possibility also exists to generate IR rovibrational emissions, such as the 4.3-μm ν_3 bands of CO_2 or the 5.3-μm fundamental and the 2.7-μm overtone bands of NO [*Whalen et al.*, 1985]. However, the long lifetimes of the IR radiating states (~ 0.1 s) compared to the duration of the transient QE fields makes QE heating relatively ineffective in producing IR emissions.

On the other hand, it has recently been realized that, even under the quasi-steady conditions between lightning discharges, TC fields can maintain the ionospheric electrons in a heated state [*Inan et al.*, 1996]. Although the quiescent fields penetrating to ionospheric altitudes are relatively smaller than the transient fields which produce sprites, they are nevertheless believed to heat electrons significantly [*Pasko et al.*, 1996]. In this paper, we consider one of the possible consequences of such steady and sustained heating, namely the steady-state excitation of IR emissions.

To determine the amount of sustained heating at 70-90 km altitude, it is necessary to model self-consistently the penetration of TC electric fields E to the upper atmosphere. Previous considerations of this problem [*Park and Dejnakarintra*, 1973; *Tzur and Roble*, 1985; *Roble*, 1991; *Velinov and Tonev*, 1995] have not accounted for the nonlinear dependence on $|E|$ of the ionospheric-electron conductivity $\hat{\sigma}_e$ due to electron heating. Here we use the recently developed two-dimensional self-consistent electrostatic heating (ESH) model of *Pasko et al.* [1996] to determine the E-field penetration and the resultant electron heating. An important consequence of the heating is the excitation of non-radiating N_2 vibrational levels, which we determine quantitatively as a function of altitude. The N_2 vibrational energy transfers efficiently to CO_2 ν_3 vibrational states, which then radiate at 4.3 μm. We use the calculated N_2 vibrational excitation rates in the ARC non-LTE radiative-transfer code [*Wintersteiner et al.*, 1992; *Nebel et al.*, 1994] to determine CO_2 ν_3 excitation and the resultant IR emission levels.

N_2 Vibrational Excitation

The ESH model of *Pasko et al.* [1996] assumes cylindrical symmetry about the z-axis (altitude) and describes the steady-state (that is, static) electric field established in the atmosphere due to a vertical TC dipole charge configuration, consisting of two charges of $+Q$ and $-Q$ separated in altitude above a perfectly conducting ground at $z = 0$. The E field is calculated using the stationary charge continuity equation, in which TC charges play the role of steady current sources, assumed to be maintained against conduction loss by external means, for example updrafts or other meteorological processes. The nonlinear heating effects on $\hat{\sigma}_e$ of the medium above the TC are calculated self-consistently by solving the nonlinear continuity equation.

Each of the dipole charges $\pm Q$ is taken to be distributed in the form of spherical or disk-shaped clouds centered at altitude $z_o^{\pm}$ and of width $2a$. The spherical distributions have positive and negative charge densities $\propto e^{-[(z-z_o^{\pm})^2+r^2]/a^2}$, where r is the radial cylindrical coordinate, a=3 km, z_o^-=5 km, and z_o^+=15 km. For disk-shaped TC charge distributions, such as those which exist in a mesoscale convective system (MCS) [for example, *Marshall et al.*, 1996], the charge density is $\propto e^{-[(z-z_o^{\pm})^2]/a^2}$ (a=3 km) and is uniform in the r direction out to the radius of the disk. Larger E fields will result everywhere above the cloud if either z_o^+ or $|z_o^+ - z_o^-|$ is increased.

An important parameter that determines the penetration of the TC fields to high altitudes is the scale height of the upper-atmospheric conductivity σ. At altitudes below ~60 km, the atmospheric conductivity is largely determined by the ion component σ_i, which is not significantly modified by ESH. Nevertheless, altitude profiles of σ_i are not well known, especially above an active thunderstorm, and available *in situ* data from rockets [for example, *Hale et al.*, 1981] indicate large variability. Accordingly, we provide results for different ambient σ_i profiles. At altitudes above ~60 km, the electron component $\hat{\sigma}_e$ is dominant. Although the ambient profiles of electron density are also not well known, results are less sensitive to the assumed ambient profiles in this altitude range, since the electron conductivity is reduced self-consistently by ESH. The electrostatic fields penetrating to high altitudes are generally of low intensity, so that neither ionization effects nor excitation of optical emissions need be considered. Note that the type of coupling considered here occurs during the entire duration of the thunderstorm, including the times between lightning discharges.

With the electrostatic field self-consistently determined as a function of altitude, the electron distribution function is readily estimated using a kinetic formulation [*Taranenko et al.*, 1993] by accounting for all electron collisional losses,

[1]Phillips Laboratory / Geophysics, Hanscom AFB, Mass.
[2]STAR Laboratory, Stanford University, Stanford, Calif.
[3]ARCON Corporation, Waltham, Mass.

Paper number 97GL02753.
0094-8534/97/97GL-02753$05.00

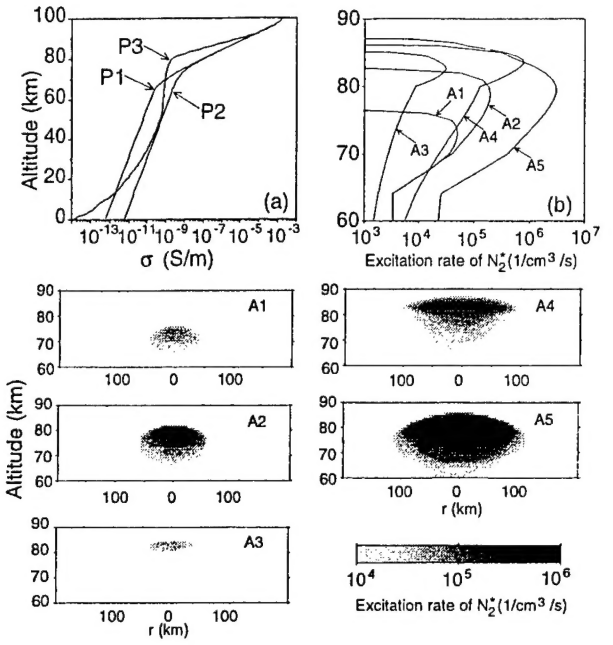

Figure 1. (a) Three models of ambient electrical conductivity σ. (b) Altitude profiles and (c) spatial distributions of N_2(v) excitation rate due to heated electrons.

including the very important loss due to vibrational excitation of N_2. The excitation rates for N_2(v) can then be determined using well-known cross sections [*Phelps*, 1987]. For numerical calculations, we use parametrized production rates of vibrationally excited N_2 as a function of E/N (where E is the electric field and N is the neutral number density) [*Pasko et al.*, 1997].

We consider three different nighttime ambient conductivity profiles P1, P2, and P3 (Figure 1a). Profile P1 consists of an ion conductivity profile with a constant scale height of 11 km and an electron conductivity calculated from a typical D-region electron-density profile used in previous work [*Inan et al.*, 1996]. Profile P2 has the same scale height as P1, but has an ionic conductivity ten times larger at each altitude. Profile P3 is probably the most 'typical' midlatitude profile and is based on a range of rocket measurements [*Hale*, 1994, and references therein]. Profiles P1 and P2 bracket the range of variations of σ at altitudes ~60 km.

We combine the three different conductivity profiles with the two different TC charge configurations into five cases which span the range of interest. The five cases are: (i) A1 - spherical, $Q = \pm 100$ C, σ profile P1; (ii) A2 - same as A1, but with σ profile P2; (iii) A3 - same as A1, but with σ profile P3; (iv) A4 - disk-shaped, radius = 50 km, $Q = \pm 1000$ C, σ profile P3; and (v) A5 - same as A4, but with σ profile P2. TC charges of 100 C are not uncommon [for example, *Brook et al.*, 1982]. Moreover, the effective surface charge density corresponding to 1000 C spread over a disk with radius 50 km is ~130 nC/m^2, several times lower than the values of 400-1200 nC/m^2 suggested by *Marshall et al.*[1996] for a MCS. Thus, the TC charge magnitudes used in our calculations are quite conservative.

Figure 1b shows altitude profiles (at r=0) of the vibrational excitation rate of N_2(v) corresponding to the different cases. The lateral extent of the regions which are excited are indicated for each case separately in the panels of Figure 1c. Comparison of results for Cases A2 and A1 illustrate that higher conductivity values at lower altitudes (Case A2) allow for better upward penetration of fields and higher field values. However, the most effective coupling is obtained for disk-like TC charge distributions as represented by A4 and A5. The largest perturbations are produced for Case A5, which also provides for the penetration of the electrostatic field to the highest altitude. In Cases A4 and A5 electric fields $E \sim$ 1-10 V/m are produced near z = 80 km. Such fields are too low to produce significant ionization. In all cases electron densities are near ambient values.

CO_2 ν_3 Vibrational Temperatures

We determine the populations of the ν_3 excited states using a line-by-line non-LTE model [*Wintersteiner et al.*, 1992], in which rate equations for the level populations and the equation of transfer for the radiative flux are solved simultaneously. The extended duration of the TC fields makes it possible to use a steady-state formulation, which ignores transient radiative behavior. We consider the combined effects of electron collisional excitation and the ambient nighttime production/loss processes of *Nebel et al.* [1994].

In steady state, the main pathway for CO_2 ν_3-state excitation by heated electrons is indirect, involving vibration-to-vibration (V-V) transfer from electron-excited N_2(v), calculated in the previous section. This follows from (i) the abundance of N_2, (ii) the long lifetime of the N_2(v>0) states, and (iii) the efficient near-resonant V-V transfer process. The near-resonance requires that the rate equations be solved simultaneously for the $CO_2(\nu_3)$ and N_2(v) excited-vibrational-state populations. The stored N_2 vibrational excitation is initially transferred, with a time constant of a few seconds at 70 km to a minute at 90 km, to CO_2 ν_3 vibrational states, which then radiate rapidly at 4.3 μm (lifetime ~2.5 ms). However, in the mesosphere the effective CO_2 excited-state lifetime and the N_2(v) relaxation time are both lengthened considerably by radiation trapping and by the reverse V-V process, whereby the vibrational excitation is passed back to N_2. Effective N_2(v) relaxation times are in the range 5-7 min at 70-90 km altitude [*Kumer*, 1977].

While the vibrational energy is redistributed locally by V-V transfer, it is also being redistributed nonlocally by radiative transport. We allow vertical radiative transfer, but neglect horizontal radiative transport/diffusion of the excitation, since the horizontal scale (lateral extent of the TC charge) is much larger than the vertical scales (neutral-density and enhanced-E-field scale height). At 80 km altitude, radiation will only diffuse horizontally a few km in 20 min, negligible compared to the width of the charge distribution. Moreover, one must include in the computation a number of weaker isotopic and hot bands, since they account for most of the radiative redistribution of the excitation over altitude and most of the limb radiance at 80 km TH, the stronger bands being severely self-absorbed.

In our model calculations, we consider four CO_2 isotopes and five excited states. We include the most abundant 626 isotope, along with the minor isotopes 636, 627, and 628, and the excited states 00011, 01111 (which radiates the first hot band), and the states we shall call Group I (10011, 10012, and 02211). The notation for the CO_2 states and isotopes is given by *Nebel et al.* [1994] and by *Rothman et al.* [1992]. We assume (1) nighttime conditions, (2) a midlatitude model atmosphere similar to the U.S. Standard Atmosphere (1976), (3) non-overlapping spectral lines, and (4) local rotational equilibrium within a band at the kinetic temperature T. We express non-LTE vibrational populations in terms of a vibrational temperature T_{vib} [*Nebel et al.*, 1994].

The altitude profiles of T_{vib} were calculated for all bands of interest, and representative profiles are shown in Figures 2a-c for the unheated atmosphere and Cases A4 and A5, respectively. Results for Cases A1-A3 are not shown since enhancements were small. In each case, the T profile is shown, as well as T_{vib} profiles for N_2(v=1) and five CO_2 states. In the ambient case we see that $T_{vib} > T$ for the strongly non-LTE CO_2 states in the mesopause region, since the production is dominated by radiative excitation. The less abundant isotopes are vibrationally hotter because they are optically thinner and are excited by radiation originating further away near the warm stratopause. In the lower thermosphere, on the other hand, $T_{vib} < T$ for the CO_2 states because radiative loss (cooling to space) dominates. The T_{vib} profile for N_2 is locked to the CO_2 00011 626 T_{vib} in the mesosphere due to the strong V-V transfer. On the other hand, in the thermosphere it is locked to T, because the time constant for V-V transfer becomes very long and the N_2(v) loss is then dominated by collisions with O.

When the electrons are heated, enhancements of T_{vib} occur above 70 km and are strongest at 80 km near the peak of N_2(v) excitation by electrons. The enhancements are quite modest (~10 K) for Case A2 (not shown), but approach 50

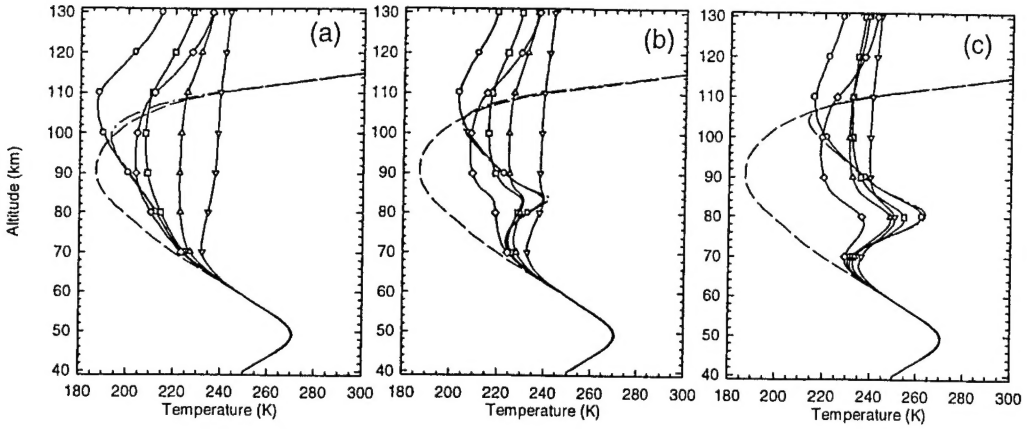

Figure 2. Altitude profiles of T_{vib} (a) for unheated conditions, (b) for Case A4, and (c) for Case A5. Symbols designate CO_2 isotopes and states as follows: ○ (626 00011), □(636 00011), △ (628 00011), ▽ (627 00011), ◇ (626 01111). Profiles of T (dashed) and N_2(v=1) T_{vib} (dash/double-dot) are also shown.

K for Case A5. An increase of 10 K (50 K) corresponds to a factor of ~2 (~17) increase in the upper-state population at T_{vib} = 220 K. A significant feature of the enhancements is that they occur not only in the region of enhanced N_2(v) excitation below 85 km, but extend up into the thermosphere, well above 130 km. The responsible mechanism is IR radiative diffusion of the excitation upward from the region of enhanced production. A similar process is effective in redistributing auroral electron energy deposited in N_2 vibration [*Winick et al.*, 1988]. The 626 and 636 01111 states also show significantly enhanced T_{vib}, but the Group I excited-state enhancements (not shown) are negligible.

CO_2 4.3-μm Limb Radiance

We now calculate the enhanced 4.3-μm radiance in limb view for LOS with tangent points located at r=0. The calculation includes segments on both the near and far side of the tangent point where ambient conditions prevail.

Figure 3a shows the nighttime limb radiance profiles for Cases A4 and A5 and for ambient conditions, for a sensor with an infinitesimal field-of-view and a wide spectral passband (4.1-4.5 μm). Cases A1-A3 (not shown) are nearly indistinguishable from the ambient, but enhancements of up to ~20% and ~100% occur for cases A4 and A5, respectively. Near-peak enhancements occur over a broad range of TH from ~76 km to >120 km, extending well above the region of E-field-enhanced production. Figure 3b shows the enhancement ratio for individual bands as a function of TH for Case A5, demonstrating that the enhancement profile depends strongly on the band. The altitude dependence is much stronger for the 626 00011-00001 (main) band, since its optical thickness prevents radiative diffusion of the enhanced production. On the other hand, the two strongest minor bands, 636 00011-00001 and 626 01111-01101, have broader enhancement profiles, due to the increased radiative diffusion. Near the altitude of peak vibrational excitation (~80 km), the main-band enhancement dominates, while in the lower thermosphere the two weaker bands have enhancements nearly equal to each other and to the main band. Although the main-band radiance is larger by as much as a factor of six at ~80 km, it only accounts for 5-10% of the radiance there, since it is severely self-absorbed. This is illustrated in Figure 3c, which shows the fraction of the total limb radiance under ambient conditions originating from the main 626 band, all of the isotopic 00011-00001 bands, the first 626 hot band, and other hot bands (largely first hot bands of minor isotopes and bands arising from Group I states). The main 626 band makes the largest contribution only below 62 km and above 105 km, while the minor-isotope 00011-00001 bands dominate the radiance from 73 to 105 km.

The variation in optical thickness of the bands and the dependence of the enhancement ratios on TH lead to interesting spectral behavior, which may be detectable with a limb-looking narrowband multichannel radiometer or with an IR spectrometer. In Figure 4 we show typical spectra for the ambient atmosphere and for Case A5 at 80 km TH. The spectrum is plotted for an instrumental resolution of 2 cm^{-1} and shows considerable structure, including band origins, sharp Q-branches, and broader P- and R-branches. It is clear that spectral-radiance enhancements are dependent on wavenumber and that diverse spectral features are enhanced differently. While the integrated radiance more than doubles, the increase within limited spectral regions, such as the 'blue spike' region near 2380 cm^{-1}, can be con-

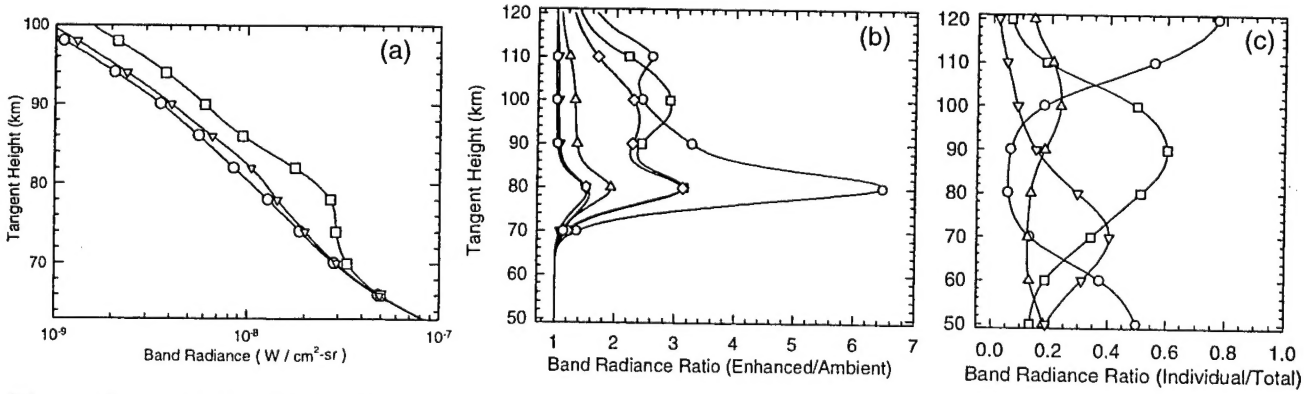

Figure 3. (a) Total limb radiance profiles for ambient nighttime and Cases A4 and A5. (b) Heating enhancement ratios for limb radiance in a number of bands versus TH for Case A5. Symbols for upper states of bands same as in Figure 2, except that curve is added (hexagons) for hot bands originating in states other than 626 01111. (c) Profiles of fractional limb radiance in certain band groups for ambient nighttime. Upper (radiating) level designations are: ○ (00011 626), □(00011 minor isotopes), △ (626 01111 hot band), ▽ (states radiating other hot bands).

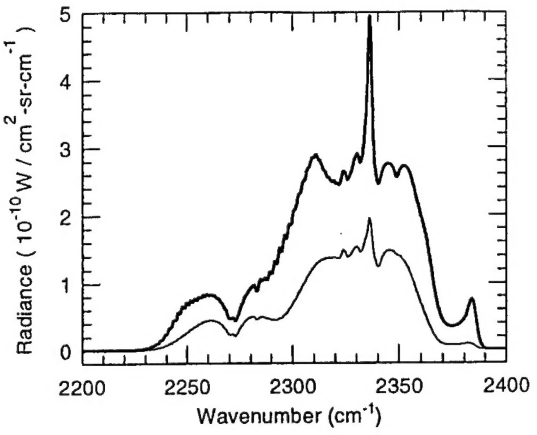

Figure 4. 4.3-μm limb spectra for TH = 80 km: Ambient night (thin), Case A5 (thick).

siderably larger. Larger effects are also possible when the heated region is on the side of the tangent point nearer the sensor.

Summary and Discussion

Our results indicate that sustained heating of lower ionospheric electrons by TC fields, as suggested by *Inan et al.* [1996], may lead to the production of detectable enhancements of 4.3-μm CO_2 emission. Model calculations for five different cases indicate that the strongest effects are expected for laterally extensive TC charge distributions, such as those associated with a MCS, and in cases where the atmospheric conductivity allows penetration of the electrostatic field to relatively high altitudes. Enhancements of CO_2 T_{vib} start near 70 km, with maximum enhancement of up to 50 K near 80 km altitude. As a result of IR-mediated radiative diffusion, the enhancements extend up into the thermosphere, well above 130 km, despite the fact that significant heating occurs only below 90 km. Limb-view broadband 4.3-μm enhancements of up to a factor of two above ambient nighttime levels are predicted for TH between 77 km and 120 km, with larger enhancements in selected narrower spectral regions. Somewhat larger enhancements would be expected if electron excitation of other molecular vibrational states were allowed, including direct excitation of CO_2 ν_3 and perhaps excitation of O_2(v), which is coupled to CO_2 ν_3 and N_2(v).

The fact that significant IR enhancements are only predicted to occur for Cases A4 and A5 underscores the dependence of the upward penetration of TC field on the profile of σ. Simple considerations of the E-field variation in an inhomogeneous medium indicate that effective penetration to ionospheric altitudes is maximized when the fewest e-foldings of σ occur between TC and ionosphere. Our results indicate that significant IR enhancements should occur when the σ profile lies in the range between P2 and P3. In view of the scarcity of *in situ* data, it is difficult to assess the geophysical conditions under which the conductivity profile would be similar to that described by profiles P2 or P3. However, rocket measurements [*Hale*, 1994] do indicate profile P3 to be a 'typical' mid-latitude nighttime profile. Thus we can reasonably expect that conditions leading to effective coupling and IR enhancements should occur at least some of the time.

The importance of having a spatially extensive MCS with area $\sim 10^4$ km^2 for obtaining E fields sufficient to excite N_2(v) is borne out by the rocket measurements of *Kelley et al.* [1985], showing E fields of only tens of mV/m above relatively small storm cells with horizontal extents $\sim$ 10-20 km, in contrast to the 1-10 V/m resulting from our calculations for charge distributions similar to those observed by *Marshall et al.* [1996]. The difference in E fields between relatively small cells and a MCS is demonstrated by U-2 aircraft measurements near $z = 20$ km over a large active storm [*Blakeslee et al.*, 1989]. These measurements reported E = 1-7 kV/m, in agreement with our calculations for Cases A4 and A5, but greater than the balloonborne measurements associated with the rocket campaign of *Kelley et al.* [1985] at 21 km by a factor of 10^3 - 10^4.

Acknowledgments. We gratefully acknowledge the sponsorship of the Air Force Office of Scientific Research's Directorate of Mathematics and Geosciences and the encouragement of L. S. Jeong and W. A. M. Blumberg. Three of us (U.S.I., V.P.P., and P.P.W.) were supported under contracts with the Phillips Laboratory, Geophysics Directorate.

References

Blakeslee, R. J., H. J. Christian, and B. Vonnegut, *J. Geophys. Res., 94*, 13135-13140, 1989.
Brook, M., M. Nakano, P. Krehbiehl, and T. Takeuti, *J. Geophys. Res., 87*, 1207, 1982.
Hale, L. C., C. L. Croskey, and J. D. Mitchell, *Geophys. Res. Lett., 8*, 927, 1981.
Hale, L. C., *J. Geophys. Res., 99*, 21089, 1994.
Hampton, D. L., M. J. Heavner, E. M. Wescott, and D. D. Sentman, *Geophys. Res. Lett., 22*, 89, 1996.
Hays, P. B. and R. G. Roble, *J. Geophys. Res., 84*, 3291, 1979.
Inan, U. S., V. P. Pasko, and T. F. Bell, *Geophys. Res. Lett., 23*, 1067-1070, 1996.
Kelley, M. C., C. L. Siefring, R. F. Pfaff, P. M. Kintner, M. Larsen, R. Green, R. H. Holzworth, L. C. Hale, J. D. Mitchell, and D. Le Vine, *J. Geophys. Res., 90*, 9815-9823, 1985.
Kumer, J. B., *J. Geophys. Res., 82*, 2203, 1977.
Marshall, T. C., M. Stolzenburg, and W. D. Rust, *J. Geophys. Res., 101*, 6979- 6996, 1996.
Mende, S. B., R. L. Rairden, G. R. Swenson, and W. A. Lyons, *Geophys. Res. Lett., 22*, 2633, 1995.
Nebel, H., P. P. Wintersteiner, R. H. Picard, J. R. Winick, and R. D. Sharma, *J. Geophys. Res., 99*, 10409-10419, 1994.
Park, C. G., and M. Dejnakarintra, *J. Geophys. Res., 78*, 6623, 1973.
Pasko, V. P., U. S. Inan, and T. F. Bell, *J. Atm Terr. Phys.*, in review, 1996.
Pasko, V. P., U. S. Inan, T. F. Bell, and Y. N. Taranenko, *J. Geophys. Res., 102*, 4529, 1997.
Phelps, A. V., *Gaseous Dielectric, 5*, 1-9, 1987.
Roble, R. G., *J. Atm. Terr. Phys., 53*, 831, 1991.
Rothman, L. S., *et al.*, *J. Quant. Spectrosc. Radiat. Transfer, 48*, 469-507, 1992.
Taranenko, Y. N., U. S. Inan, and T. F. Bell, *Geophys. Res. Lett., 20*, 1539-1542, 1993.
Tzur, I., and R. G. Roble, *J. Geophys. Res., 90*, 5989, 1985.
Velinov, P. I., and P. T. Tonev, *J. Atm. Terr. Phys., 57*, 687, 1995.
Whalen, J. A., R. R. O'Neil, and R. H. Picard, The aurora, in *Handbook of Geophysics and the Space Environment*, edited by A. S. Jursa, Chapter 12, Air Force Geophys. Lab., Bedford, Mass., 1985.
Winick, J. R., R. H. Picard, R. D. Sharma, R. A. Joseph, and P. P. Wintersteiner, in R. Rodrigo, J. J. Lopez-Moreno, M. Lopez-Puertas, and A. Molina eds., *Progress in atmospheric physics*, pp 229-237, Kluwer Academic Publ., Dordrecht, Neth., 1988.
Wintersteiner, P. P., R. H. Picard, R. D. Sharma, J. R. Winick, and R. A. Joseph, *J. Geophys. Res., 97*, 18083-18117, 1992.

R. H. Picard and J. R. Winick, PL/GPOS, Hanscom AFB, MA 01731 (e-mail: picard@plh.af.mil, winick@pldac.plh.af.mil)
U. S. Inan and V. P. Pasko, STAR Laboratory, Stanford University, Stanford, CA 94305 (e-mail: inan@star.stanford.edu, pasko@nova.stanford.edu)
P. P. Wintersteiner, ARCON Corporation, 260 Bear Hill Road, Waltham, MA 02154 (e-mail: winters@arcon.com)

(Received May 14, 1997; revised July 30, 1997; accepted August 21, 1997.)